ACS Catalysis

Perspective

pubs.acs.org/acscatalysis

Mechanism of the Catalytic Conversion of Methanol to Hydrocarbons

Samia Ilias and Aditya Bhan*

Department of Chemical Engineering and Materials Science, University of Minnesota, Twin Cities, 421 Washington Avenue SE, Minneapolis, Minnesota 55455, United States

ABSTRACT: The discovery of the dual aromatic- and olefin-based catalytic cycles in methanol-to-hydrocarbons (MTH) catalysis on acid zeolites has given a new context for rationalizing structure−function relationships for this complex chemistry. This perspective examines six major chemistries involved in the hydrocarbon pool mechanism for MTH—olefin methylation, olefin cracking, hydrogen transfer, cyclization, aromatic methylation, and aromatic dealkylation—with a focus on what is known about the rate and mechanism of these chemistries. The current mechanistic understanding of MTH limits structure−function relationships to the effect of the zeolite framework on the identity of the hydrocarbon pool and the resulting product selectivity. We emphasize the need for assessing the consequences of zeolite structure in MTH in terms of experimentally measured rates and activation barriers for individual reaction steps and in terms of speciation preferences within the dual olefin- and aromatic-catalytic cycles to alter their relative propagation. In the absence of individual reaction rates, we propose using ethene/isobutane selectivity as a measure to describe the relative rates of propagation for the aromatic- and olefin-based cycles.

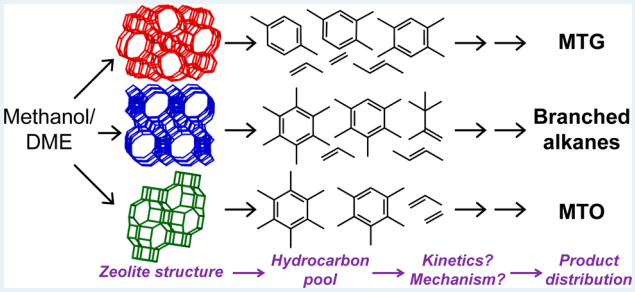

KEYWORDS: *methanol-to-hydrocarbons, methanol-to-olefins, hydrocarbon pool, zeolite, propene, methylation, cracking*

1. INTRODUCTION

As global energy demand increases simultaneously with dwindling supplies of conventional petroleum resources, nontraditional carbon-based feedstocks will be essential to supply the world with fuels and chemicals. The methanol-to-hydrocarbons (MTH) process over acid zeolite catalysts, first discovered by Mobil Research Laboratories in 1976,[1] has seen renewed interest in recent years both for its ability to grow carbon chains and because methanol can be produced via a syngas intermediate from any gasifiable carbon-based feedstock, such as natural gas,[2] coal,[3,4] and biomass.[5,6] Methanol or its dehydration product dimethyl ether (DME) can be used as a feed to produce several different classes of hydrocarbons, including light olefins (methanol-to-olefins, MTO),[7−9] gasoline-range hydrocarbons (methanol-to-gasoline, MTG),[1] branched alkanes,[10,11] and aromatics.[12] The selectivity to any of these classes of compounds is determined both by the zeolite topology and the operating conditions used.

Since the discovery of MTH, there has been much debate regarding two aspects of the chemistry: (1) the origin of the first C−C bond and (2) the mechanism by which MTH proceeds. In the past decade, a broad consensus has emerged on the inability of methanol adsorbed within the zeolite pores to couple directly at rates relevant for steady-state MTH catalysis.[13] Lesthaeghe and co-workers[14,15] used ONIOM methods to calculate activation energies and rate constants for multiple pathways to form C−C bonds starting from two methanol molecules and found activation energy barriers for direct C−C coupling to be prohibitively high (~200 kJ mol^{-1}). Experiments using fractionally distilled methanol demonstrated that the catalyst induction period for MTH on H-ZSM-5 and H-SAPO-34 is highly sensitive to the impurity concentration in the methanol feed, indicating that if direct C_1 coupling does occur, it operates at a rate significantly slower compared with the rate at which trace impurities initiate the reaction.[16] Direct C−C coupling mechanisms also require C−H bond activation; however, Marcus et al. found that feeding d_3-DME over H/D-SAPO-34 (in which 50% of the acid sites were H^+ and the other 50% were D^+) at 623 K resulted in an effluent containing approximately 25% d_0-DME, 50% d_3-DME, and 25% d_6-DME. The binomial distribution of D atoms in DME showed that C−H activation and, thus, direct C−C coupling does not occur.[17]

Early work in MTH postulated an autocatalytic mechanism on the basis of the observed catalytic induction period during which increasing the concentration of hydrocarbons greatly increased the rate of methanol/DME conversion.[1] Ono and Mori[18] first showed the co-catalytic effect of co-processing ethene and *cis*-2-butene with methanol, reducing the catalyst induction period by a factor of 2 and 4, respectively, compared with the reaction of methanol alone over H-ZSM-5 at 512 K. Additionally, Langner et al.[19] noted that by co-feeding methanol with higher alcohols that readily dehydrate to linear olefins under reaction conditions on H-ZSM-5, the kinetic induction period could be substantially reduced, indicating the important catalytic role of olefins in MTH. Dessau and LaPierre[20,21] outlined a reaction mechanism for MTH based on

Received: October 6, 2012
Revised: November 25, 2012
Published: December 5, 2012

   dx.doi.org/10.1021/cs3006583 | ACS Catal. 2013, 3, 18−31

Scheme 1. Dual Olefin and Aromatic Methylation Catalytic Cycle for Methanol to Hydrocarbons on H-ZSM-5[a]

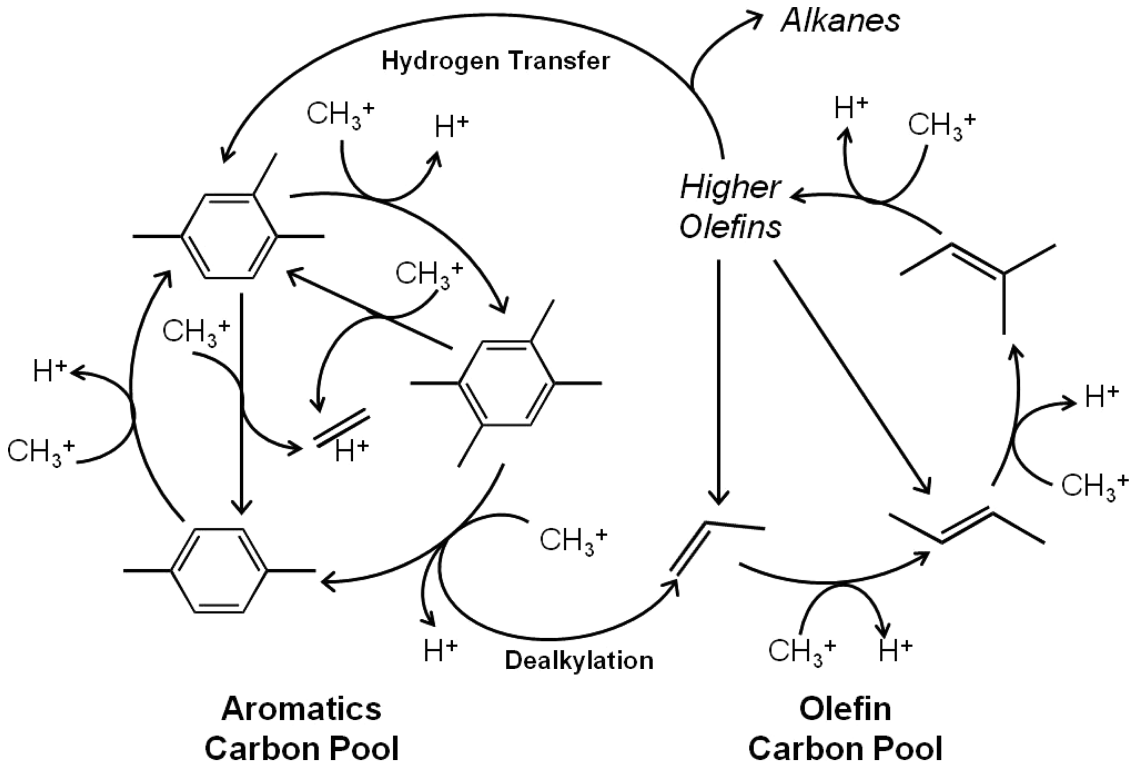

[a]Adapted from Ref 87.

olefins that are sequentially methylated and subsequently crack to form smaller olefins or participate in hydrogen transfer reactions to form alkanes and aromatics. However, Langner et al.[19] showed that co-feeding cyclohexanol with methanol also significantly reduced the catalyst induction period, indicating that both olefins and cyclic species play a critical role in MTH.

Dahl and Kolboe proposed a "hydrocarbon pool" mechanism in which methanol forms a pool of $(CH_2)_n$ species within the zeolite pores that produces light olefins, alkanes, and aromatics.[7−9] It is now widely agreed upon that MTH proceeds through this indirect hydrocarbon pool mechanism, though our understanding of the hydrocarbon pool identity has evolved. By reacting a series of two 20-μL pulses of methanol over H-SAPO-34, Haw and co-workers[22] showed that methylbenzenes can act as organic co-catalysts for MTO, increasing methanol conversion from 14% to 100% between the first and second pulse. Mole et al.[23] observed the incorporation of ^{12}C atoms from toluene into ethene when ^{12}C-toluene was co-reacted with ^{13}C-methanol over H-ZSM-5. Similar observations were made by Mikkelsen et al.[24] on H-BEA and H-MOR, providing further evidence that polymethylbenzenes are active hydrocarbon pool species for light olefin formation. Additionally, Davis and co-workers[25] observed that the isotopologue distribution of ethene was distinct from other olefins when ^{14}C-methanol was co-processed with ^{12}C-labeled C_{3+} alcohols on H-ZSM-5, suggesting that the mechanism of ethene formation is different from higher olefin formation. Isotopic switching experiments by Svelle, Bjorgen, and co-workers[26,27] on H-ZSM-5 in which ^{12}C-methanol feed is switched with ^{13}C-methanol feed during steady-state reaction showed that ^{13}C incorporation of ethene closely matched that of methylbenzenes, and the ^{13}C incorporation of C_{3+} olefins matched each other. This result showed that two catalytic cycles are at work in MTH on H-ZSM-5: one that involves methylbenzenes and ethene and another that involves C_{3+} olefins (Scheme 1). Similar work has since been done on various other zeolites and zeotype materials, though often with the purpose of showing the dominance of one cycle over another.[28−32]

The emergence of this dual cycle mechanism has contributed significantly to the general understanding of the hydrocarbon pool mechanism. Previous mechanistic understanding of MTH provided a relationship between zeolite topology and MTH product distribution in very specific cases, such as SAPO-34 (CHA framework), which has narrow 8-MR openings that hinder diffusion of molecules larger than linear C_4 hydrocarbons out of the 12-MR cages, and ZSM-22 (TON framework), in which narrow 10-MR pores hinder aromatic dealkylation reactions. For other zeolite frameworks, structure−function relationships have not been fully developed; however, the dual cycle mechanism for MTH provides a new context for understanding speciation preferences in the hydrocarbon pool for a given zeolite. Elucidating the identity of the hydrocarbon pool on various zeolites now provides further insight into how zeolite topology affects the MTH product distribution, but as Scheme 2 shows, the missing steps include an understanding of the kinetic behavior of hydrocarbon pool species and how the kinetics of these species affects the available mechanistic pathways and selectivity.

2. CHEMISTRY OF MTH

Six major chemistries occur within the dual cycle mechanism for MTH: (1) olefin methylation, (2) olefin cracking, (3) hydrogen transfer, (4) cyclization, (5) aromatic methylation, and (6) aromatic dealkylation. The rate and role of each of these chemistries in determining the product distribution of MTH is an outstanding question. Below, we discuss what is

dx.doi.org/10.1021/cs3006583 | ACS Catal. 2013, 3, 18−31

Scheme 2. The Current Understanding of MTH Has Focused on Making a Direct Connection between Zeolite Structure and Product Distribution

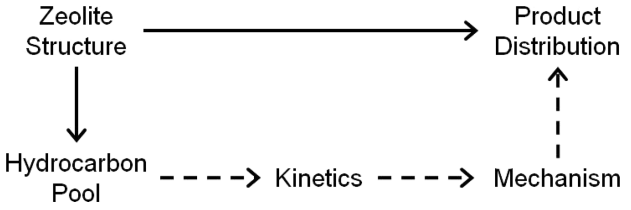

known about the kinetics, mechanism, and effect of zeolite structure on these chemistries and postulate a research perspective on linking zeolite structure to MTH product distribution.

2.1. Olefin Methylation. Scheme 1 shows that olefin methylation is one route by which methyls are incorporated into hydrocarbon products. Work by Cui et al.[33,34] on ZSM-22 (TON framework) and subsequent work by Teketel et al.[28,35,36] on ZSM-22 and ZSM-23 (MTT framework) has shown that some unidimensional 10-MR zeolites hinder both the transport of cyclic species out of the zeolite pore and aromatic dealkylation reactions. The olefin methylation pathway dominates in these zeolites, resulting in a product distribution rich in C_{5+} aliphatics at temperatures above 623 K. There are two proposed mechanisms for olefin methylation (Scheme 3): (1) a co-adsorbed mechanism in which methanol and an olefin are adsorbed on a single acid site and react in a single, concerted step; and (2) a surface methoxide mechanism in which methanol or DME dehydrates to form a methoxide that desorbs upon reaction with an olefin. Although evidence supporting both mechanisms has recently been reviewed,[37] we examine the consequences of methanol dimer formation on these two mechanisms.

Scheme 3. A Representation of the Surface Methoxide Mechanism (left) and Co-adsorbed Mechanism (right) for Olefin Methylation with Methanol

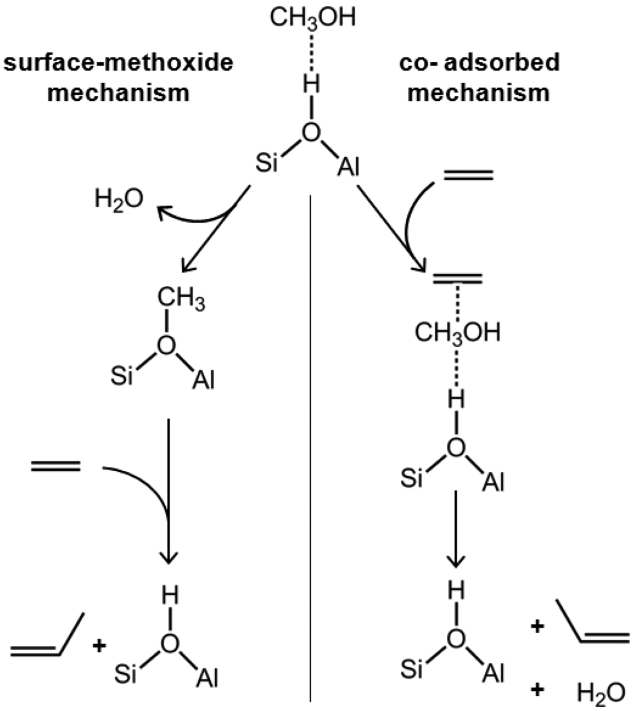

The kinetics of C_2-C_4 olefin methylation has been studied on H-ZSM-5 using ^{13}C-methanol by Svelle et al.[38,39] and using DME on H-ZSM-5, H-BEA, H-FER, and H-MOR by Hill et al.[40−42] Despite these reactions taking place over a large range of experimental conditions (320−713 K), both studies show that olefin methylation has a first-order dependence on the olefin pressure and a zero-order dependence on the methylating agent (methanol or DME) and that this kinetic behavior is consistent across the zeolite frameworks studied.[38−42] The zero-order dependence on the methylating agent shows that the catalyst surface is saturated with the methylating agent, although the identity of the methylating agent (physisorbed methanol/DME or surface methoxide) is debated. Rate constants for C_2-C_4 olefin methylation on H-ZSM-5 are summarized in Figure 1. Although all four zeolites investigated by Hill et al. have similar activation barriers for propene and butene methylation, pre-exponential factors and methylation rates are an order of magnitude higher for H-ZSM-5 and H-BEA compared with H-MOR and H-FER, indicating that olefin methylation reactions are propagated to different extents, depending on the identity of the zeolite framework.[40−42] Across the four zeolites reported, olefin methylation rate constants increase and activation barriers systematically decrease with increasing olefin size, indicating that the relative stability of reaction intermediates increases with increasing carbon chain length.[38−42] Hill et al. also measured olefin methylation rates for all four butene isomers in the absence of C_4 isomerization reactions on H-ZSM-5 and H-BEA, observing that the rate constant of isobutene methylation was an order of magnitude greater than that of the other butene isomers.[40] These observations are consistent with the conclusion that the reactivity of olefins is dependent on the degree of substitution about the double bond, which stabilizes intermediate carbocations through inductive electron donation. Similarly, Bercaw, Labinger, and co-workers[43−46] show for methanol conversion over ZnI_2 and InI_3 in the liquid phase and Iglesia and co-workers[10,11,47] show for DME conversion over H-BEA that under conditions when skeletal isomerization is suppressed (<500 K), highly branched alkenes and alkanes, particularly triptane and triptene, are the dominant product as a result of methylation reactions favoring the formation of the most substituted carbenium ion as a reaction intermediate.

Computational chemistry studies using DFT on 30−46T cluster sizes to account for dispersion effects have also investigated C_2-C_4 olefin methylation via the co-adsorption mechanism and, in agreement with experimental work, show that activation energy barriers decrease while rate constants increase systematically with olefin size (Figure 1).[48,49] Additionally, rate constants and activation energy barriers match reasonably well with experimental work (within a factor of 2 for ethene and propene methylation rates).[48] A recent DFT study by Mazar et al. has investigated the pathway for ethene methylation via a surface methoxide intermediate on H-ZSM-5, H-FER, H-BEA, H-MOR, and H-CHA.[50] The reaction of a surface methoxide with ethene on all zeolite frameworks and acid site locations investigated proceeds via two distinct transition states, one in which a cyclopropane-like species is formed and a second that involves ring-opening of the cyclopropane-like species. The apparent activation energy barriers for the surface methoxide mechanism ranged from 97 to 141 kJ mol^{-1},[50] which compares well with apparent

dx.doi.org/10.1021/cs3006583 | ACS Catal. 2013, 3, 18−31

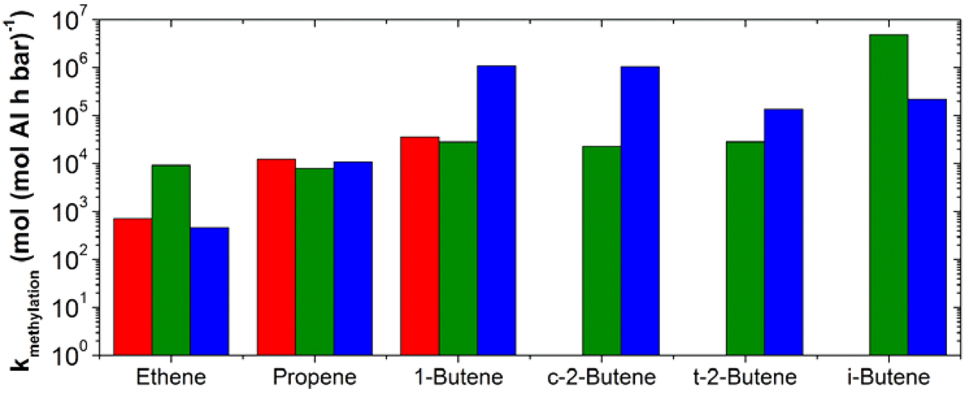

Figure 1. Rate constants at 623 K for C_2−C_4 olefin methylation on H-ZSM-5 from (red) refs 38 and 39 (experimental), (green) refs 40−42. (experimental), and (blue) ref 48 (computational, co-adsorbed mechanism).

activation energy barriers calculated for the co-adsorption mechanism on H-ZSM-5 (94−104 kJ mol^{-1})[48,49] as well as experimental values (98−109 kJ mol^{-1}).[39,41,42]

The co-adsorbed mechanism requires the simultaneous adsorption of both methanol and an olefin on a single Brønsted acid site. Hybrid MP2/DFT calculations with periodic boundary conditions for a full unit cell of H-ZSM-5 show that the initial adsorption of methanol (−115 kJ mol^{-1}) is stronger than the subsequent co-adsorption of the olefin (−37, and −53 kJ mol^{-1} for ethene and propene, respectively), and the co-adsorption enthalpy for ethene with methanol is reduced by only 2 kJ mol^{-1} if a purely siliceous framework was used instead of H-ZSM-5, which contained one Al/unit cell.[49] This result shows that van der Waals interactions with the zeolite pore walls are the dominant factor in ethylene co-adsorption, as opposed to interactions with the Brønsted acid site. In addition to methanol−olefin co-adsorption complexes, methanol dimer co-adsorption complexes may also form at the Brønsted acid site. Lesthaeghe et al. calculated the enthalpy of methanol dimer adsorption to be −117 kJ mol^{-1} using ONIOM calculations on 30T and 46T clusters at 720 K on H-ZSM-5,[51] in agreement with microcalorimetry measurements by Lee and Gorte,[52] showing the differential heat of adsorption of methanol on H-ZSM-5 at 400 K to be −115 kJ mol^{-1} for up to 2 methanol molecules per acid site. The enthalpy of adsorption for methanol dimers is similar to the enthalpy of adsorption for methanol−olefin complexes (−152 and −168 kJ mol^{-1} for ethene and propene complexes, respectively);[49] hence, methanol dimer formation may compete with the formation of methanol−olefin co-adsorbed complexes. Stich et al.[53] found that the activation of methanol is facile in the absence of hydrogen bonding using first-principle molecular dynamics simulations, suggesting that methanol dimers would be inactive for methylation of olefins. Therefore, the formation of methanol−olefin co-adsorption complexes would be inhibited by the formation of inactive methanol dimer complexes, and correspondingly, increasing the methanol pressure would result in inhibition of olefin methylation rates.

Unlike larger alkoxide species, surface methoxides lack a β-H and are therefore unable to desorb as olefins. As a result, surface methoxides are stable intermediates and have been observed on a variety of zeolites via in situ infrared spectroscopy (with bands at 2980 and 2968 cm^{-1} for asymmetric and symmetric stretching, respectively)[18,54−56] and ^{13}C MAS NMR spectroscopy (with a signal at 56 ppm).[22,57−59] Boronat et al.[60] investigated surface methoxide formation applying DFT-D to 130 atom clusters of the 12-MR channel of H-MOR and found intrinsic activation barriers to be 139 and 150 kJ mol^{-1} for DME and methanol precursors, respectively. In comparison, other DFT studies on 3−4T clusters calculate the barrier for methoxide formation from methanol to be >200 kJ mol^{-1};[61−63] hence, the inclusion of dispersion effects is critical in determining if surface methoxide species are formed during olefin methylation reactions. Once formed, surface methoxides have been shown to be reactive with a variety of molecules, including, but not limited to, toluene, alkyl halides, and aniline on frameworks such as H−Y, SAPO-34, and H-MOR.[55,58,59,64] Additionally, Marcus et al.[17] fed d_3-DME over SAPO-34 at 573 K, and Hill et al.[42] fed a 50:50 mixture of unlabeled DME with d_6-DME over H-ZSM-5 at 393 K, and both groups observed a DME effluent dominated by d_0, d_3, and d_6 isotopologues, indicating that methoxide formation is rapid and facile at experimental conditions relevant for MTH. Post-reaction water titration of reactions of DME with butene result in a 1:1 ratio of CH_3OH/Al, providing further evidence of surface methoxide formation during steady-state olefin methylation reactions.[40]

Olefin methylation has also been investigated on H-SAPO-34 at 673 K by Dahl and Kolboe.[7−9] Co-feed experiments of ^{13}C-methanol with ^{12}C-ethanol (2 methanol/1 ethanol molar ratio), which dehydrates readily to form ethene under reaction conditions, show that at early times-on-stream (<40 minutes), 20% of propene in the effluent came from ethene methylation, containing only one ^{13}C atom.[8] Similarly, when ^{13}C-methanol was co-reacted with ^{12}C-isopropyl alcohol (3 methanol/1 isopropyl alcohol molar ratio), which dehydrates to form propene, 24% of *trans*-2-butene came from propene methylation.[9] The low fraction of propene and *trans*-2-butene isotopologues containing only one ^{13}C atom shows that olefin methylation is not the dominant route for propene and butene formation on H-SAPO-34; rather, aromatic dealkylation reactions are responsible for light olefin formation.[22]

2.2. Olefin Cracking. Olefin cracking as a route to light olefin production in MTH was first proposed by Dessau and LaPierre[20,21] and is a route used commercially to increase production of propene in Lurgi's methanol-to-propene (MTP) process, which is based on using H-ZSM-5 formulations. The mechanism of olefin cracking requires protonation of an olefin to form an alkoxide intermediate, followed by β-scission of the alkoxide to form a smaller olefin and a smaller alkoxide. The smaller alkoxide subsequently desorbs to form another olefin and leaves behind a proton to regenerate the acid site.

dx.doi.org/10.1021/cs3006583 | *ACS Catal.* 2013, 3, 18−31

Scheme 4. Different Modes of β-Scission for C_8 Isomers with Nomenclature Developed by Weitkamp et al.[65] and Buchanan et al.[66]

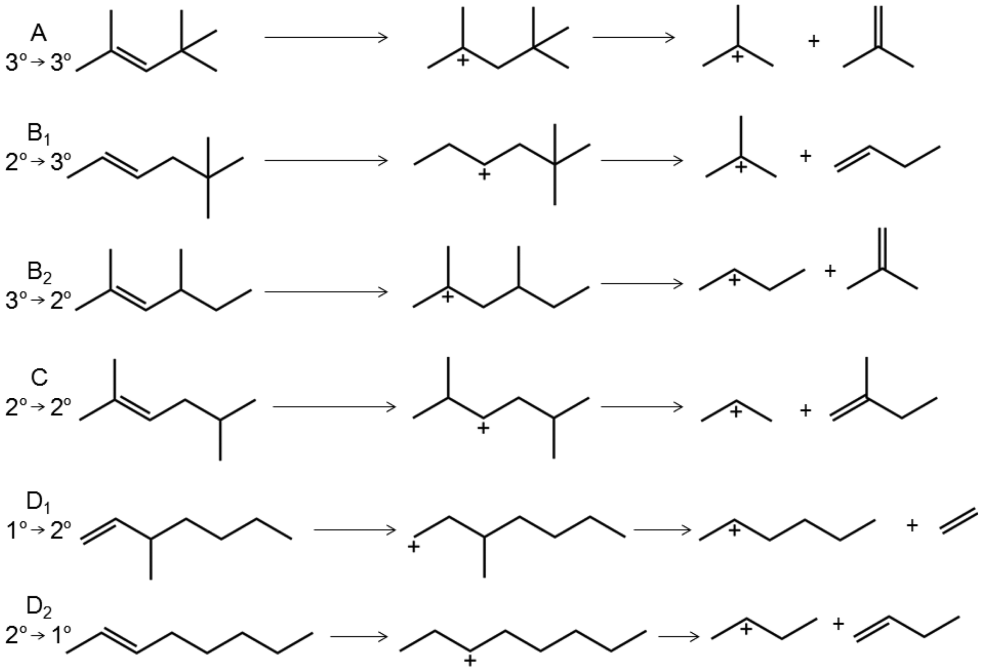

Weitkamp et al.[65] first developed nomenclature to describe the various modes of cracking based on carbenium ion types for products and reactants, a useful method for understanding the difference in cracking rates as a function of olefin size and skeletal structure. Buchanan et al.[66] extended this nomenclature (Scheme 4) in a study on the relative rates of monomolecular alkene cracking for C_5−C_8 olefins on H-ZSM-5 at 783 K. First-order rate constants for cracking were reported, with relative rates of C_5:C_6:C_7:C_8 alkene cracking to be 1:24:192:603. A near-equilibrium distribution of hexene isomers was achieved at 26% conversion of 1-hexene feed, and the reaction of three different skeletal isomers of heptene resulted in identical product distributions, suggesting that numerous adsorption, isomerization, and desorption events take place prior to and are significantly faster than β-scission.[66] The dominant mode of cracking for hexene was 2° → 2°, whereas for heptenes and 1-octene, it was 2° → 3° and 3° → 2°, respectively. In contrast to 1-octene, 2,4,4-trimethyl-2-pentene cracked 50 times more slowly, even though this branched isomer cracked through a more energetically favored 3° → 3° cracking mode. The slower reaction rate of 2,4,4-trimethyl-2-pentene compared with 1-octene is mostly likely due to diffusion limitations of this molecule in H-ZSM-5.

Speciation of olefin isomers is critical in determining the product selectivity for MTH. For example, if olefin cracking is considerably faster than olefin methylation, then the product distribution should be rich in light olefins. In contrast, if olefin cracking is slower than olefin methylation, then the product distribution may be rich in larger olefins, which may cyclize to eventually form aromatics. Simonetti et al.[11] measured the rates of β-scission for a variety of C_5−C_8 alkene isomers while co-feeding ^{13}C-DME on H-BEA at 473 K and found that in general, the rate of β-scission is at least 40 times slower than olefin methylation and is of the same order of magnitude as skeletal isomerization. The exception was 3,4,4-trimethyl-2-pentene (344T2P): β-scission for this C_8 isomer was almost twice as fast as olefin methylation, most likely because 344T2P is able to form a stable tertiary carbenium ion transition state. As a result of this facile cracking pathway, 344T2P is removed from the product distribution of MTH on H-BEA at these conditions.

Using 3T clusters at the B3LYP/6-31++G** level of theory, van Santen and co-workers[67−69] found three possible pathways for β-scission of 1-butoxide and 2-pentoxide: (1) a one step path with a ringlike transition state, (2) a two-step pathway involving a hydrogen-bonded transition state with a substituted cyclopropane (pathway HBCP), and (3) a one-step pathway with a hydrogen-bonded transition state. Their calculations showed that pathway HBCP had the lowest activation energy barrier. In this pathway, a new C−C bond is formed, resulting in the formation of a substituted cyclopropane species that subsequently undergoes cleavage of two different C−C bonds to form an olefin and an alkoxide. Activation energies were found to decrease with increasing carbon number; however, the activation energies reported are overestimated (>230 kJ mol^{-1}) because of the small cluster sizes used.[67,68]

In an independent study using 3T clusters at the HF/6-31G* level of theory, Hay et al.[70] studied the effect of branching on β-scission and found that the activation energy barrier for the β-scission of 2-pentoxide was 20−25 kJ mol^{-1} higher than for the β-scission of 2-methyl-2-pentoxide. At 773 K, this difference in activation energy barriers corresponds to rates for C_6 β-scission being 20−50 times faster compared with C_5 β-scission, assuming that both reactions have similar pre-exponential factors. This ratio of C_6 to C_5 β-scission rates is in agreement with experimental work by Buchanan et al.[66] Elucidating rates of β-scission on various zeolites will be key in determining what fraction of light olefins, particularly propene and butenes, are products of the aromatic- vs. olefin-based carbon pool; however, the prevalence of secondary reactions, such as olefin oligomerization and dehydrocyclization, hinder the measurement of kinetic parameters of β-scission.

dx.doi.org/10.1021/cs3006583 | ACS Catal. 2013, 3, 18−31

2.3. Hydrogen Transfer. The dehydrative condensation of CH_3OH (= CH_2 + H_2O) should lead to the formation of olefins $(CH_2)_n$; however, the observed product distribution for MTG consists predominantly of saturated alkanes and aromatic compounds. The formation of alkanes requires that an equivalent of H_2 be supplied, which concurrently results in the formation of hydrogen-deficient species, such as dienes; trienes; and, for MTH, polymethylbenzenes. A stoichiometric correlation between the yield of saturated alkanes and the yield of methylbenzene compounds is noted in both homogeneous and heterogeneous catalyzed C_1 homologation. Hydrogen transfer reactions therefore, alter the relative number of chain carriers available for the olefin- and aromatic-based cycles in MTH.

Hydrogen transfer is a bimolecular reaction in which a hydrogen atom is transferred between an adsorbed surface alkoxide and a cyclic or acyclic alkane or alkene. Because this involves the abstraction of a hydrogen atom and is mediated by carbocationic transition states, as inferred from DFT calculations, branched alkanes are facile hydrogen donors compared with linear alkanes because the resulting carbocationic transition states are more stable.[71−74] Alkenes with tertiary allylic C−H bonds are even more reactive hydrogen donors than branched alkanes because they delocalize positive charge more effectively, which leads, in turn, to more stable carbocations. Davis and co-workers[75] co-fed ^{14}C-labeled methylcyclohexane and methanol on H-ZSM-5 in a 1:70 molar ratio at 583 K and noted that the toluene formed in MTH was not predominantly ^{14}C-labeled, suggesting cycloalkanes were poor hydrogen donors under MTH reaction conditions. This observation regarding hydrogen transfer from cyclic molecules under MTH conditions is consistent with our discussion of cyclization mechanisms (section 2.4), where we suggest that ring closure in MTH predominantly occurs for C_8^+ species and also suggests that under low-temperature conditions (<548 K), light alkanes and cyclic alkanes may be considered as termination products of MTH.

The hydrogen transfer index (HTI), defined as the ratio of alkanes to alkenes formed, has also been used to qualitatively infer the influence of zeolite structure on the rate of hydrogen transfer with the inference being that methanol, $(CH_2)H_2O$, dehydrates to form olefins $(CH_2)_n$ which disproportionate to form alkanes (C_nH_{2n+2}) and aromatics. Hence, the ratio of alkenes to alkanes is a measure of hydrogen transfer characteristics of the zeolite structure. Early work from Mikkelson et al.[12] and more recent work from Teketel et al.[35] for zeolites with one dimensional 10-MR channels have continued to use this description; however, as discussed by Mikkelson, the HTI ratio depends on the time-on-stream and deactivation characteristics as well as chemical conversion. This method is limited in its description of hydrogen transfer simply because hydrogen transfer is a bimolecular reaction and the number and identity of species that can undergo hydrogen transfer is changing with conversion, and therefore, the rate of hydrogen transfer varies with conversion. The HTI descriptor concept attempts to qualitatively describe an average of the hydrogen transfer rate and cannot be used to infer either coking or deactivation characteristics of the zeolite.

Inferring mechanistic details and kinetic parameters regarding hydrogen transfer from experiments requires the isolation of surface alkoxides on zeolites and experimental conditions such that bimolecular hydrogen transfer steps occur predominantly in the absence of competing alkylation, oligomerization/β-scission, and isomerization steps. This challenge has largely precluded experimental studies; however, a significant advancement has resulted from low-temperature (~473 K) methanol homologation studies using ZnI_2 and InI_3 catalysts in the homogeneous phase[43−46,76] and from H-BEA[10,11,47] catalyzed low-temperature (423−473 K) synthesis of branched hydrocarbons.

Bercaw, Labinger, and co-workers[43−46,76] have investigated the mechanism of methanol conversion to branched hydrocarbons on iodide-based homogeneous catalysts to show that the remarkable selectivity to high-octane triptyl compounds can be explained on the basis of (i) methylation and deprotonation preferentially leading to the most highly substituted carbocations and (ii) the relative rate of hydrogen transfer to methylation being greater for triptene than its precursors. They probed the relative rates of olefin methylation to hydrogen transfer by co-feeding olefins with 1 equiv of 1,4-cyclohexadiene (CHD), which is expected to be a particularly good hydrogen donor. A systematic study of olefin substitution comparing behaviors of 2,3-dimethyl-2-pentene, 2,4-dimethyl-2-pentene, 2,4-dimethyl-1-pentene, and triptene—olefins that all contain seven carbon atoms and roughly similar steric properties, but differing degrees of substitution about the double bond—revealed that the addition of CHD resulted in at least a 20-fold reduction in the ratio of C_8 methylation products to that of C_7 alkanes formed via hydrogen transfer, mostly likely from CHD.[76] In the absence of a hydrogen donor such as CHD, the source for hydrogen transfer must be the olefin itself; the cyclic diene, CHD, was therefore 20 times as proficient at hydrogen transfer as the acyclic monoolefins. It was also noted that the ratio of methylation (based on the yield of C_8 products) to hydrogen transfer (based on the yield of C_7 alkanes) was highest for the tetrasubstituted alkene, 2,3-dimethyl-2-pentene, decreasingly markedly for the trisubstituted and again for the disubstituted isomers, suggesting that the rate of methylation to hydrogen transfer and, therefore, chain growth (methylation) to chain termination (hydrogen transfer) varies systematically with the degree of olefin substitution.[76]

In a series of related studies on zeolite-based heterogeneous catalysts for methanol/dimethyl ether (DME) homologation to branched hydrocarbons at low temperature (~473 K) and high DME pressure such that the olefin-based cycle in MTH dominates over the aromatic-based cycle, Iglesia and co-workers[11,47] have attempted to quantify the rate of methylation versus the rate of hydrogen transfer reactions in experiments involving a co-feed of ^{13}C-DME with various ^{12}C-labeled C_4−C_7 olefins. The rate of hydrogen transfer for DME homologation intermediates of a given chain length and carbon backbone structure was determined from the rate of formation of the unlabeled alkane corresponding to the added unlabeled alkene. The rate of methylation of each alkene co-feed was assessed from the rate of formation of all molecules containing at least one ^{12}C atom, except those containing only ^{12}C atoms. The authors further define the ratio of the rate of hydrogen transfer to the sum of the rates of methylation and hydrogen transfer as β and attempt to rationalize the variation in β depending on the carbon chain length and branching of the olefin. High β values therefore represent fast hydrogen transfer and slow methylation. The authors observe that β values involved in acid-catalyzed C_1 homologation can be rationalized on the basis of carbocation stability of the transition state complexes, with hydrogen transfer to tertiary alkoxides being

dx.doi.org/10.1021/cs3006583 | ACS Catal. 2013, 3, 18−31

Scheme 5. Possible Pathways for 1-Hexene and 1,5-Hexadiene Cyclization on Acid Zeolites with Activation Energy Barriers (kJ mol^{-1}) Based on DFT/MM Level Calculations on 138 T sites[84] and 2-Layered ONIOM(B3LYP/6-31+g(d):HF/6-31+g(d) Calculations[85]

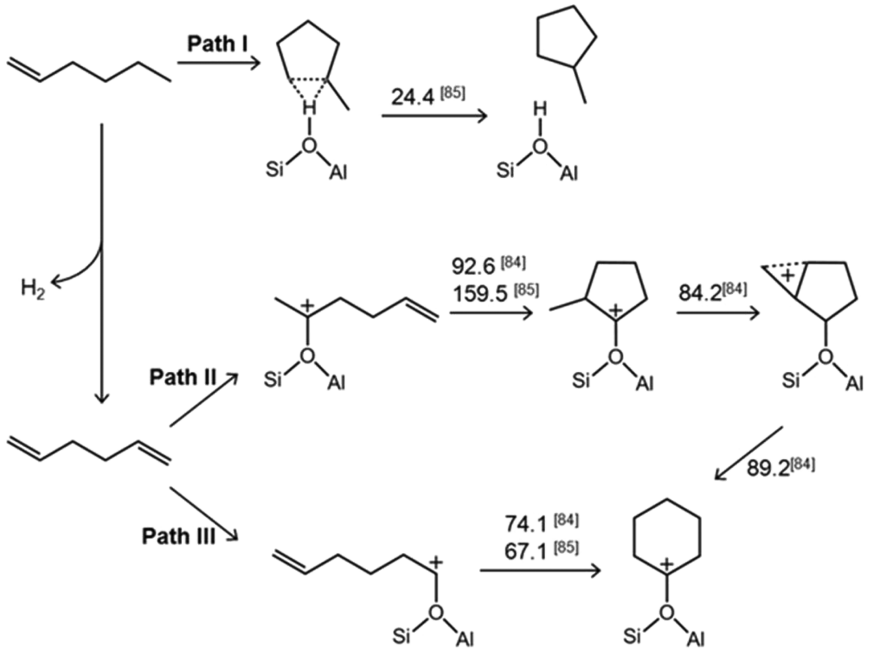

favored and low termination probabilities of alkenes with alkyl substituents at both C atoms resulting from stable transition states for methylation.[11] Intraparticle concentration gradients and high reactivity of olefins make accurate measurements of hydrogen transfer rates difficult; however, the definition of β precludes the need to measure these concentrations, since it contains a ratio of methylation and hydrogen transfer rates, which are both proportional to alkene concentrations.

The addition of adamantane as a hydrogen transfer co-catalyst has been shown for both homogeneous[46] and heterogeneous[47] catalyzed low-temperature methanol/DME homologation to result in co-homologation of alkanes with a marked increase (>10 fold) in the incorporation of C atoms from the alkane in the presence of adamantane. Because dehydrogenation of adamantane is not possible, it acts as a reversible hydrogen shuttle and facilitates dehydrogenation of alkanes to alkenes and terminates chains formed in methylation via alkoxide desorption as alkanes instead of as alkenes. The addition of such hydrogen transfer co-catalysts and the co-processing of alkanes provide distinct strategies to change the number of olefin and alkane chain carriers in MTH and to satisfy the stoichiometric requirements of forming thermodynamically favored alkanes without the formation of hydrogen-deficient aromatics, which act as coke precursors. Although these recent studies clearly represent an advancement in our understanding of hydrogen transfer reactions involved in MTH, only relative rates of hydrogen transfer under specific reaction conditions that do not include a description of the identity or reactivity of the co-reactant in hydrogen transfer elementary steps has been described. For instance, the β parameter described by Iglesia and co-workers[47] is noted to increase with increasing olefin pressure (β increases by a factor of ~2−3, depending on the identity of the olefin when olefin pressure is increased from 0.5 to 3.7 kPa). These effects of olefin pressure on β indicate that olefins influence hydrogen transfer rates more strongly than methylation rates, even though both rates are expected to depend linearly on olefin pressure. Olefins upon dehydrogenation by hydrogen transfer form multiply unsaturated olefins and cyclic compounds that are presumably even more efficient at hydrogen transfer; however, the identity and reactivity of such molecules eludes experimental probes prior to their subsequent dehydrogenation to form aromatics.

Computational density functional theory (DFT) and ab initio studies have played a seminal role in elucidating the mechanism of elementary hydrogen transfer steps on zeolitic acids. Early work from Kazansky and co-workers[67,71,72,77] examined hydrogen transfer reactions for systems involving surface alkoxides and alkanes with reactant and product states comprising alkoxides (1° → 1°, 2° → 2°, 3° → 2°, 3° → 3°) adsorbed on the surface on 1T clusters at the MP2(fc)//6-31++G*//HF/6-31G** level of theory. The geometry and charge of the carbocationic transition state in these studies closely resembled a nonclassical penta-coordinated carbonium ion species. At the transition state, the alkoxide and alkane are connected by a central hydrogen atom with a small positive or even negative charge; hence, the hydridic character of the reaction. Corma and co-workers[73,74,78,79] extended the scope of these studies by proposing a common intermediate for hydride transfer, disproportionation, and alkylation reactions between adsorbed alkoxides and alkanes based on DFT calculations (B3PW91/6-31G*) done on 3T clusters. Periodic DFT calculations from Neurock and co-workers[80] postulated a relatively flat potential energy surface; however, they also predicted carbenium-ion-like transition states and shared hydride species as lower-energy intermediates. On this basis, the authors postulate that carbenium ion stability is expected to correlate with selectivity to hydrogen transfer versus alkylation and oligomerization. A recent study from Mullen and Janik[81] employing DFT-D methods to account for dispersion interactions in zeolites shows, in agreement with experimental studies from Bercaw and co-workers[43−46] and Iglesia and co-workers,[10,11,47] that activation energies decrease as the

dx.doi.org/10.1021/cs3006583 | ACS Catal. 2013, 3, 18−31

substitution of the hydride donor or acceptor species increases. The identity and reactivity of the specific co-reactant involved in hydrogen transfer and the dependence of catalytic rates (or relative rates) on spatial constraints remain as outstanding questions for MTH and, more generally, acid catalysis by zeolites.

2.4. Cyclization. Shown in Scheme 1, the olefin- and aromatic-based cycles are not independent of one another and "communicate" through cyclization and aromatic dealkylation steps. Cyclization is related to aromatization in that cycloalkanes and cycloolefins are not stable products of MTH and are quickly dehydrogenated to form aromatics.

There are two possible generalized routes to olefin cyclization and aromatization. One involves dehydrogenation of olefins to form dienes and trienes that undergo cyclization to aromatics. In the second route, olefins first form cycloalkanes and are subsequently dehydrogenated to form aromatics. In both of these routes, dehydrogenation occurs through hydrogen transfer reactions in which olefins or cycloalkanes donate hydrogen to other hydrocarbons that act as hydrogen acceptors. Temperature-programmed surface reaction studies of C_6−C_9 olefins on HY using mass spectroscopy show the presence of dehydrogenated intermediates of aromatics; however, it was not determined if the intermediates were dienes/trienes or their cyclic analogues.[82] Studies in which *n*-hexane and *n*-heptane were converted over H-ZSM-5 at 683 K resulted in the production of C_1−C_5 aliphatics as well as a significant yield of C_7 and C_8 aromatics (over 25 wt % for both reactants).[83] The presence of aliphatics smaller than the reactant indicates that alkane cracking is occurring simultaneously with cyclization reactions. The formation of aromatics larger than the reactant show that side reactions of cyclization, such as olefin oligomerization and alkylation of aromatics, also occur. The prevalence of secondary reactions such as these prevents experimental evidence from revealing if olefin dehydrogenation occurs prior to cyclization or vice versa.

Computational studies have investigated olefin and diene cyclization through 1,5-cyclization and 1,6-cyclization pathways on H-ZSM-5 using both embedded cluster calculations at the DFT/MM level for a 138T cluster and 2-layered ONIOM-(B3LYP/6-31+g(d):HF/6-31+g(d)).[84,85] The results of these studies are summarized in Scheme 5. The cyclization of physisorbed hexene to methylcyclopentane (Scheme 5, path I) has the lowest activation energy of the cyclization pathways shown in Scheme 5. However, because the ring expansion mechanism for the formation of cyclohexane was not studied, it is unclear if methylcyclopentane is a favorable precursor to benzene. The results in Scheme 5 also show that for 1,5-hexadiene, the pathway for 1,5-cyclization (path II) is more highly activated than that for 1,6-cyclization (path III), most likely because of the higher total charge of the transition state (0.848 au vs 0.770 au) and the longer distance between the transition state and alkoxide oxygen (3.05 Å vs 2.36 Å) for 1,5-cyclization compared with the analogue for 1,6 cyclization.[84] On the basis of the high activation energy barrier for 1,5-cyclization of hexadiene as well as for ring expansion from methylcyclopentene to cyclohexene, Joshi and Thomson concluded that 1,6-cyclization occurs for C_6 aliphatic precursors.[84]

Joshi and Thomson[86] also studied 1,6-cyclization reactions using DFT/MM for C_7 and C_8 dienes in which a secondary alkoxide intermediate is formed prior to cyclization. Their findings show that increased stability of secondary carbenium ion transition states over primary carbenium ion transitions states results in the activation energy of C_7 and C_8 diene cyclization to be 29 kJ mol^{-1} lower than C_6 diene cyclization.[86] These computational results are in agreement with experimental results that show aliphatics with more than 6 carbons are the predominant precursors to aromatics. Our recent work has shown when co-feeding ^{13}C-toluene with ^{12}C-DME at 548 K on H-ZSM-5, the toluene in the effluent as well as *o*-xylene have a very small fraction (<1%) of completely ^{12}C-labeled isotopologues (Figure 2a, b).[87] In contrast, *p*-xylene, 1,2,4-trimethylbenzene, and durene have a significant fraction of completely ^{12}C-labeled isotopologues, and this fraction increases monotonically from 9.8% to 31.8% with aromatic size (Figure 2c−e). Furthermore, when ^{13}C-propene is co-fed with ^{12}C-toluene and ^{12}C-DME, benzene and toluene are not observed as significant products (<0.5 C% selectivity), and the fraction of ^{13}C in aromatics increases with aromatic size.[87] The higher incorporation of ^{13}C atoms in C_8−C_{10} aromatics with a ^{13}C-propene co-feed and the preclusion of ^{13}C atoms in C_{8+} methylbenzenes with a ^{13}C-toluene co-feed are most likely due to cyclization occurring predominantly for C_{8+} aliphatics at 548 K. The question of when cyclization occurs on different catalysts at different conditions will need to be addressed in the future because of the importance of cyclic species in MTH.

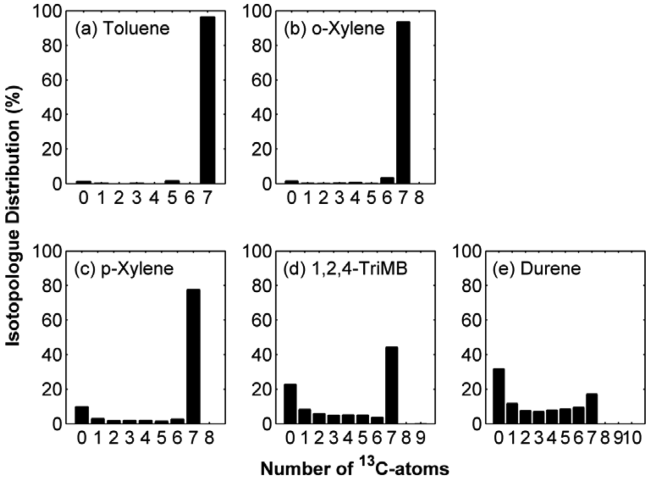

Figure 2. ^{12}C/^{13}C isotopologue distributions for (a) toluene, (b) *o*-xylene, (c) *p*-xylene, (d) 1,2,4-trimethylbenzene, and (e) durene for the reaction of 70 kPa ^{12}C-DME (WHSV = 15.5 g (g catalyst h)$^{-1}$) with 4.1 kPa of ^{13}C-toluene at 548 K over H-ZSM-5. Adapted from ref 87.

2.5. Aromatic Methylation. Aromatics, specifically polymethylbenzenes, play a crucial role in MTH catalysis in that these species, along with olefins, act as scaffolds for methylation. Isotopic labeling studies of methanol co-fed with an aromatic show that aromatic methylation reactions involve sequential methylation steps; however, varying incorporation of ^{13}C atoms into methylbenzenes also shows that aromatic methylation is not the only route by which methylbenzenes are formed.[24,87−89]

Similar to olefin methylation, there are two proposed mechanisms for aromatic methylation: a stepwise mechanism and a co-adsorbed mechanism. In the stepwise mechanism, methanol or dimethyl ether first dehydrates as the Brønsted acid site to form a surface methoxide, which then methylates aromatics in a Rideal-type mechanism. In the co-adsorbed

dx.doi.org/10.1021/cs3006583 | ACS Catal. 2013, 3, 18−31

Scheme 6. A Representation of the Paring and Side-Chain Methylation Mechanism for Olefin Elimination from Hexamethylbenzene with the Zeolite Represented as Z-H or Z^- in Its Protonated or Deprotonated Form, Respectively[a]

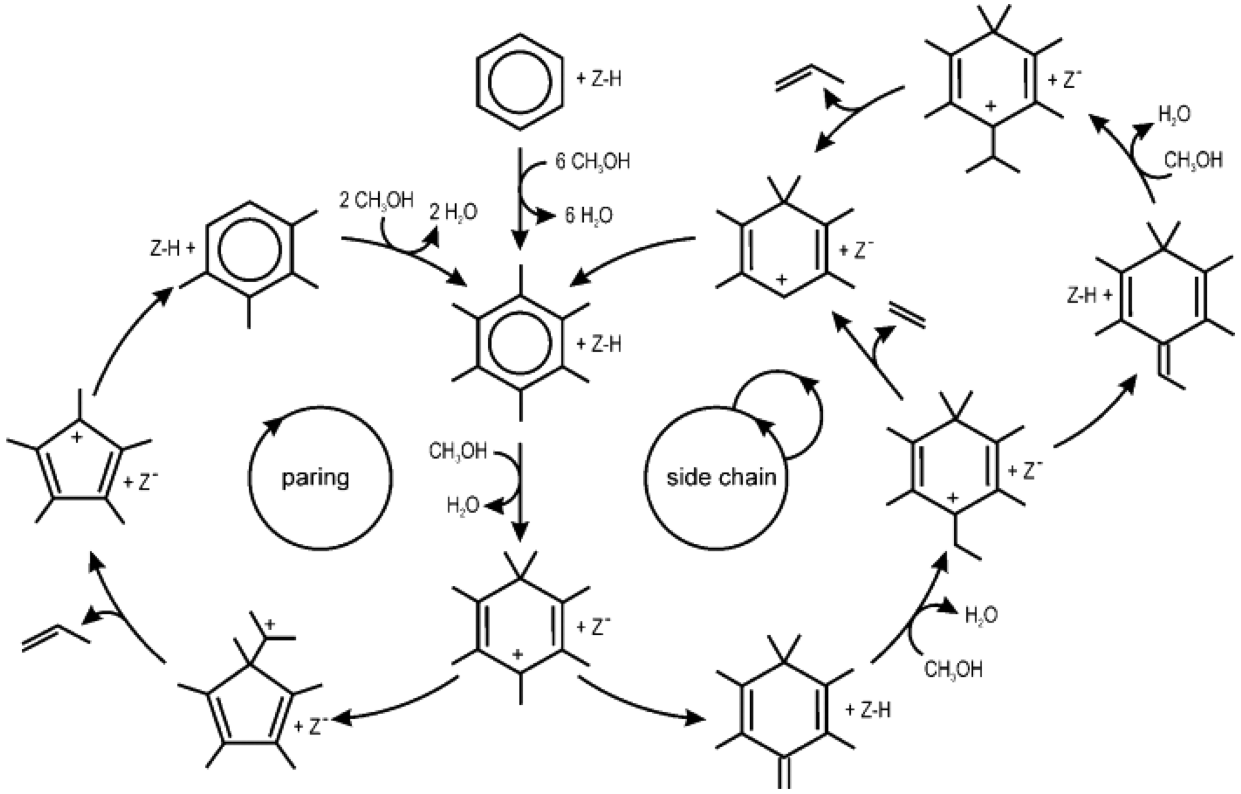

[a]Reproduced with permission from ref 114.

mechanism, methanol or dimethyl ether and the aromatic form a co-adsorbed complex at the acid site and form the methylated product in a single, concerted step. A discussion on the surface methoxide mechanism and co-adsorption mechanism has already been presented in Section 2.1 on olefin methylation and is also applicable to aromatic methylation. To extend the discussion in Section 2.1 to aromatics, Mirth and Lercher[90] showed that at 473 K on H-ZSM-5, toluene/methanol co-adsorbed complexes decompose under 10^{-6} mbar vacuum first by toluene desorption, followed by incomplete methanol desorption, monitored with infrared spectroscopy and mass spectrometry. The incomplete desorption of methanol under vacuum is consistent with the formation of surface methoxide species. In contrast, Saepurahman et al.[91] observed using infrared spectroscopy that during steady-state benzene methylation on H-ZSM-5, the band for Brønsted acid sites (3595 cm^{-1}) remained unchanged and methoxides on Brønsted acid sites were not observed after the first few minutes of reaction, which would be consistent with the co-adsorbed mechanism.

Much of the previous work on aromatic methylation has focused on toluene methylation, and we briefly summarize some of these results with a focus on H-ZSM-5. DFT calculations for 4T clusters estimate the intrinsic activation energy of toluene methylation to be 180−195 kJ mol^{-1}, with methylation proceeding through a co-adsorption complex.[92−95] ONIOM calculations on 46T clusters of H-ZSM-5 estimate a lower barrier of ∼162.5 kJ mol^{-1}.[96] In comparison, most experimental work on H-ZSM-5 shows that the apparent activation energy of toluene methylation is between 50−80 kJ mol^{-1}.[97−99] Estimating the enthalpy of adsorption to be ∼80 kJ mol^{-1} for low loadings of toluene on H-ZSM-5,[100,101] the intrinsic activation energy for toluene methylation on H-ZSM-5 based on experimental work is in the range of 130−160 kJ mol^{-1}.

A recent kinetic and DFT study[89,91] has shown that the kinetics of benzene methylation on both H-ZSM-5 and H-BEA vary little with topology. Benzene methylation on both zeolites exhibits a zero-order dependence on methanol partial pressure, activation energies between 56−58 kJ mol^{-1}, and rate constants within a factor of 3.7 at 623 K.[89,91] Activation energy barriers of gem-methylation of hexamethylbenzene on H-ZSM-5 (126 kJ mol^{-1}), H-BEA (144 kJ mol^{-1}), and H−CHA (60.8 kJ mol^{-1}) have been calculated using ONIOM methods[102] and imply that the similarity in benzene methylation kinetics and rate constants for H-ZSM-5 and H-BEA does not necessarily indicate that aromatic methylation in general is similar for both catalysts. It is probable that aromatic methylation kinetics differ significantly for larger methylbenzenes as their kinetic diameters approach the zeolite pore diameter. Although the elucidation of benzene methylation kinetics is an important step in understanding aromatic methylation, we surmise that barriers to methylation will vary as the aromatic species size approaches the size of the zeolite pore, and a systematic study of reactions kinetics in absence of intraparticle mass transfer and secondary reactions will be critical in understanding the crossover for aromatics from active hydrocarbon pool species to coke precursors. Obtaining the kinetic behavior of methylbenezenes in the absence of intraparticle mass transfer will, in turn, require an assessment of methylbenzene diffusion in zeolite pores.

dx.doi.org/10.1021/cs3006583 | ACS Catal. 2013, 3, 18−31

2.6. Aromatic Dealkylation. SAPO-34, a catalyst that is used commercially in UOP/Norsk Hydro's MTO process,[103−106] forms light olefins almost exclusively through aromatic dealkylation, showing the importance of this chemistry as a route to olefin production. In a series of experiments using methanol as a reactant on SAPO-34, Song et al.[107] stopped methanol flow after a duration of time and observed the gas phase effluent with GC and the aromatics entrained within the catalyst with ^{13}C CP/MAS NMR. For these experiments, a low number of average methyl groups per benzene ring (Me_{avg}) was correlated to higher ethene selectivity compared with propene selectivity, and this trend was consistent with space velocities varying by 4 orders of magnitude, and temperatures from 673−823 K. Although this correlation of low Me_{avg} to high ethene selectivity on SAPO-34 provides insight into the precursors for ethene formation from methylbenzenes, the mechanism of olefin formation on SAPO-34, as well as on other zeolites, is unclear. Two different mechanisms have been proposed for aromatic dealkylation and are shown in Scheme 6: (1) the side-chain methylation mechanism and (2) the paring mechanism. A recent review[108] has provided a comprehensive summary of the computational literature regarding these two mechanisms; therefore, we will focus primarily on experimental evidence supporting these mechanisms. Briefly summarizing the two proposed mechanisms, in the side-chain methylation mechanism, gem-methylation of a methylbenzene species results in elimination of a methyl hydrogen, thus forming an exocyclic double bond, which can undergo side chain methylation. This side chain can then crack to form ethene or propene. The paring mechanism is also initiated by the gem-methylation of a methylbenzene, which in this mechanism results in ring contraction. An alkyl substituent is formed that, in turn, cracks to produce light olefins.

The starting point for both the paring mechanism and the side chain methylation is a gem-methylation step in which an aromatic ring carbon is doubly methylated, thus breaking aromaticity and forming a charged species. Using hexamethylbenzene as an example, gem-methylation of this species would result in the formation of a heptamethylbenzenium ion. GC/MS and NMR spectroscopy studies have shown that heptamethylbenzium ions are easily formed by co-feeding benzene with methanol on H-BEA at low temperatures (<623 K) and are easily methylated further to eventually form naphthalenes that behave as coke precursors.[88,109−112] Additionally, ONIOM calculations on 5T clusters have shown that the activation energy for gem-methylation decreases as the number of methyl groups on the benzene ring increases.[102] This trend, however, does not hold in the presence of a zeolite framework because of the effects of confinement. Calculations on 46T clusters of H-ZSM-5 show that the barrier height for gem-methylation decreases monotonically with increasing number of methyl groups for toluene, *p*-xylene, and 1,2,4-trimethylbenzene.[102] The activation energies of gem-methylation for durene, pentamethylbenzene, and hexamethylbenzene on H-ZSM-5, however, are all higher than that for 1,2,4-trimethylbenzene. The common route explored by DFT is for exocyclic methylation to occur at the para position to the *gem*-methyl group.[113,114] Lesthaeghe et al.,[115] however, assert that because aromatic cations are rigid and tend to stay close to the aluminum defect, it is more likely that exocyclic methylation occurs ortho to the *gem*-methyl group.

The paring mechanism was first hypothesized by Sullivan et al.[116] to explain the high selectivity of hexamethylbenzene conversion to isobutane on nickel sulfide on silica−alumina. The formation of a cyclopentenyl cation is a key step in this reaction mechanism. Xu and Haw[117] first provided NMR evidence for the existence of these species on zeolites in significant amounts when feeding cyclopentene over H-ZSM-5. Additional IR and NMR spectroscopic studies have also shown that cyclopentenyl cations form over various acid zeolites and are persistent cations.[118−121] In later pulse experiments, Haw et al.[122] showed that the 1,3-dimethylcyclopentyl carbenium ion forms in less than 0.5 s after one pulse of ethene (1.9 mol of ethene per acid site) is reacted on H-ZSM-5 at 623 K. The presence of this cation in the zeolite completely eliminated the induction period of dimethyl ether conversion in a subsequent pulse to the same catalyst (0.46 mol of DME per acid site). This result shows the high reactivity and co-catalytic nature of cyclopentenyl species for MTH; however, this alone does not confirm that light olefins are eliminated from these species.

One consequence of the paring mechanism that distinguishes it from the side-chain methylation mechanism is that ring contraction and subsequent olefin elimination steps result in a ring carbon from the methylbenzene being incorporated into the olefin formed. Isotopic studies in which an aromatic is co-fed with methanol/DME (with only one ^{13}C-labeled reactant) have shown that aromatic ring carbons are, indeed, incorporated into light olefins for multiple acid zeolites,[22−24,87,88,111,123] and Bjørgen et al. observed that a majority of propene and isobutane molecules (∼60%) contained only one ^{12}C atom when ^{13}C-methanol was co-fed with ^{12}C-benzene at low temperatures (523−543 K) on H-BEA.[88] Only one aromatic ring carbon was incorporated into these products, which supports the paring mechanism for olefin formation.

Another consequence of the paring mechanism is that it provides a mechanism for methyl group carbons on aromatics to become incorporated into the benzene ring. For isotopic experiments by Bjørgen et al. described above, this would result in aromatics with mixed isotopologue distributions for the benzene ring in methylbenzenes and has also been observed experimentally by various researchers on multiple acid zeolites.[21,24,87,88,123] Scrambling, however, maybe be an event independent of the paring mechanism if repeated ring contractions and ring expansions occur without the elimination of alkyl groups. This could also lead to carbons that were originally ring carbons being incorporated into olefins through the side-chain methylation mechanism.

The key intermediate of the side-chain methylation mechanism that distinguishes it from the paring mechanism is the formation of methylbenzenes that also have ethyl, propyl, or other alkyl groups. Co-reactions of ^{13}C-methanol with ^{12}C-ethylbenzene and ^{12}C-cumene at 623 K on H-BEA have shown that these species react to form significant amounts of ethene and propene, respectively.[123] Additionally, ethylbenzene alone over H-BEA was essentially unreactive, whereas cumene alone did eliminate propene, and both ethylbenzene and cumene were more reactive for olefin elimination in the presence of methanol,[123] implying that methylation of the aromatic facilitates olefin elimination. Reactions of butylbenzene isomers over H-BEA at 623 K in the absence of methanol show that reactivity of these molecules to eliminate butenes follows what would be expected for carbocation chemistry: butylbenzene isomers with tertiary and quaternary alkyl carbons neighboring the aromatic ring carbons were significantly more reactive, with

dx.doi.org/10.1021/cs3006583 | ACS Catal. 2013, 3, 18−31

conversions of 87−96% compared with isomers with secondary alkyl carbons neighboring the aromatic ring carbon, which had conversions of 10−13% under identical conditions.[124] When these butylbenzene isomers were co-reacted with ^{13}C-methanol, the isotopic distribution of C_4 alkenes and alkanes was consistent with what would be expected to be eliminated from the butylbenzene co-feed.[124] These results provide evidence that the side-chain methylation mechanism is a possible route for olefin formation from methylbenzenes.

Lesthaeghe et al.[114] investigated the activation energy required for various gem-methylated methylbenzium ions (with the positive charge located para to the *gem*-methyl group) to form gem-methylated aromatics with an exocyclic double bond located at the para position to the *gem*-methyl group using 5T cluster calculations at the B3LYP/6-31+G(d) level of theory. In general, larger methylbenzenes form more stable carbocations and are thus more difficult to deprotonate; however, the location of the methyl group relative to the *gem*-methyl group primarily determines the barrier to exocyclic double bond formation. Activation barriers increase by ∼5 kJ mol^{-1} for each additional methyl group that is para or ortho to the *gem*-methyl group.[114] ^{13}C NMR studies of methanol conversion on H-ZSM-5 by Anderson and Klinowski[125] show that although trimethylbenzene isomers are not equilibrated in the effluent, isomers adsorbed within the zeolite pores are in equilibrium with one another. In contrast, tetramethylbenzene isomers are not equilibrated within the zeolite pores or the effluent, most likely because of the narrow zeolite pores restricting isomerization reactions. Restriction of isomerization reactions within the pores of some zeolites will thus determine the relative abundance of particular methylbenzene isomers compared with others, affecting the rate at which olefin dealkylation occurs.

Isotopic switching experiments in which a ^{12}C-methanol feed is switched with a ^{13}C-methanol feed during steady-state reaction show that the isotopic distribution of ethene matches that of di-, tri-, and tetramethylbenzenes on medium-pore zeolite H-ZSM-5[26,27] and penta- and hexamethylbenzene on larger pore zeolites H-BEA[30,31] and H-SAPO-34.[29] A quantitative model of ^{13}C atom incorporation into the olefin and aromatic products at short times-on-stream after the switch could provide a valuable method for distinguishing which of these two aromatic dealkylation mechanisms occurs in MTH, as well as determining the identity of the immediate aromatic precursor to ethene and propene. Additionally, experimental rates of olefin elimination from aromatics have not been determined and would be key in understanding what fraction of light olefins formed come from the aromatic- or olefin-based cycles.

3. PERSPECTIVES

The emergence of the dual-catalytic cycle for MTH, which encompasses the six chemistries discussed here, was an important step in understanding the identity of reactive intermediates that comprise the hydrocarbon pool and in understanding how these hydrocarbon pool species contribute to the selectivity towards certain products of MTH. In this context, the effect of different zeolite or zeotype frameworks on observed product selectivity can be understood. SAPO-34 and ZSM-22 are two frameworks that can essentially be viewed as two different extremes of the dual-catalytic cycle. In SAPO-34, the aromatic-based cycle dominates because of the product shape selectivity in which the small 8-MR windows hinders C_{5+} hydrocarbons from escaping the larger 12-MR cavities, resulting in a product selectivity rich in light olefins.[7−9,29] In contrast, the unidimensional 10-MR pores of H-ZSM-22 are too small for aromatics to be reactive for olefin formation, and the olefin-based cycle dominates, resulting in a selectivity rich in C_{5+} aliphatics.[28,34−36]

The ability to relate the product selectivity of SAPO-34 and H-ZSM-22 to the catalyst topology is unique to these two zeolites. For these two catalysts, the relationship among structure, hydrocarbon pool composition, and product selectivity is easier to understand. For other zeolite structures, however, the relationship is less clear. For example, H-ZSM-5 and H-BEA can propagate both the aromatic- and olefin-based cycle, and the propagation of these two cycles is tunable.[10,24,87,108] Under the conditions employed by Mobil when MTH was first discovered (644 K and 1.0 LHSV), the product distribution over H-ZSM-5 was rich in gasoline-range alkanes and aromatics. Current interest in MTH has shifted to the production of olefins, and H-ZSM-5 has been developed as an MTP (methanol-to-propene) catalyst by Lurgi. In this process, C_2/C_4 products are recycled back to the reactor so that the final product distribution is mostly propene.[108] Work by Iglesia and co-workers has also shown that H-BEA can be used to selectively form highly branched C_4 and C_7 aliphatics by using high pressures of DME (>50 kPa) to create a catalytic surface dominated by the methylating agent coupled with low temperatures (473 K) to minimize isomerization reactions.[10,11] Using these conditions on H-BEA, the relative propagation of the olefin-based cycle is faster than the aromatic-based cycle.

The question that remains for these two catalysts and other similar zeolites is what causes one cycle to propagate faster relative to the other. Work by Olsbye and co-workers has made significant contributions in understanding how the zeolite structure affects the composition of the hydrocarbon pool species, in particular, the identity of aromatics active for olefin elimination.[26−28,30,31,36] Extending this work will require obtaining more kinetic data and mechanistic information for the various chemistries discussed within this work. By quantifying kinetics through studies similar to the work of Svelle et al.[38,39,89,91] and Hill et al.,[42] the important steps in the overall chemistry can be determined. For example, benzene, propene, and butene methylation are all faster on H-ZSM-5 than on H-BEA, but rates and kinetic parameters for aromatic dealkylation or olefin cracking are necessary to determine how much each cycle contributes to the product distribution on these two catalysts.

In the absence of detailed kinetic parameters for individual reaction steps, the relative propagation of the aromatic- to olefin-based catalytic cycles can be assessed by determining the rate and selectivity of termination products of these cycles that are predominantly unreactive in subsequent MTH reactions. One such descriptor we propose is the ratio of ethene to isobutane synthesis rates on H-ZSM-5. Kinetic studies show that ethene methylation is at least an order of magnitude slower than other olefin methylation reactions, and isotoptic switching studies show that the ^{13}C incorporation of ethene matches that of aromatics on various zeolites;[26,29,30,38,39,42] therefore, ethene can be considered to be a termination product of the aromatics-based cycle. Isotopic switching studies on H-ZSM-5 also show that the incorporation of ^{13}C atoms in isobutene matches that of other C_{3+} olefins, showing that on H-ZSM-5, isobutene is predominantly formed via the olefin-based cycle.[26,27] Isobutane can be formed from isobutene via hydrogen transfer reactions,

dx.doi.org/10.1021/cs3006583 | ACS Catal. 2013, 3, 18−31

and because alkanes are less reactive than olefins or aromatics on zeolites, isobutane can be considered a termination product of the olefin-based cycle. Our data taken from ref 87 (Figure 3)

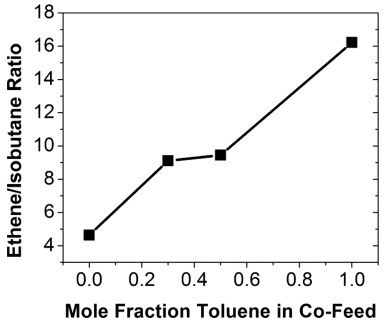

Figure 3. Ratio of ethene/isobutane selectivity (C basis) for the reactions of reaction of 70 kPa DME in the presence of a 4 kPa co-feed of varying composition of propene and toluene at 548 K over H-ZSM-5, DME WHSV = 15.5 g (g catalyst h)$^{-1}$ at iso conversion (20.8−22.7 C %).

shows that this ratio varies systematically with the amount of olefin or aromatic co-fed with DME at 548 K under isoconversion conditions (20.8−22.7 % C) on H-ZSM-5. The ratio increases as the mole fraction of toluene in the co-feed increases, thus increasing the relative propagation of the aromatic-based cycle over the olefin-based cycle. This systematic trend in the ethene/isobutane synthesis rates indicates that the relative propagation of the two cycles on H-ZSM-5 can be assessed on the basis of this ratio. Although this specific ratio may not be an appropriate descriptor for other zeolites, such as H-BEA, where prior work shows that isobutene incorporates carbons originating from aromatics,[88,111] or small-pore zeolites, in which isobutane transport may be diffusion-limited, other similar ratios may be used to describe the relative propagation of the aromatic- and olefin-based cycles. Descriptors such as ethene and isobutane are still qualitative because it is not possible to assess the rate of individual steps, but they bring us closer to a quantitative understanding of complex MTH chemistry.

4. CONCLUSION

The conversion of MTH is a complex chemistry in which aromatics and olefins act as co-catalysts that undergo repeated methylation and cracking reactions. The six chemistries discussed in this work—olefin methylation, olefin cracking, hydrogen transfer, cyclization, aromatic methylation, and aromatic dealkylation—are the major chemistries in MTH in which the dual catalytic cycle operates. For olefin methylation, olefin cracking, hydrogen transfer, and cyclization, chemistries involving olefins (or dienes in the case of cyclization), the rate of reaction and activation energy barriers strongly depended on the degree of substitution about the double bond. Longer chain lengths and more branching generally result in higher reaction rates due to the formation of more stable carbocationic transition states compared with linear alkenes. Chemistries involving aromatics are in general more space-demanding than those involving olefins; hence, steric effects of confinement within the zeolite pores can result in larger, more substituted aromatic transition states corresponding to lower reactions rates compared with smaller aromatics.

Product distributions of MTH can be understood to be the effect of zeolite topology and operating conditions causing either the aromatic- or olefin-based cycle to propagate more relative to the other cycle. Referring back to Scheme 2, the goal in understanding MTH should be developing structure−function relationships for the zeolite catalysts used in this chemistry. With the emergence of the dual cycle mechanism, the relationship between zeolite structure and product selectivity has been elucidated for a few catalysts (H-SAPO-34 and H-ZSM-22), and isotopic experiments have established the relationship between zeolite structure and the identity of aromatic hydrocarbon pool species. An understanding of the interplay between zeolite structure, identity of the hydrocarbon pool, kinetic behavior of the hydrocarbon pool species, and how kinetics affects the available mechanistic pathways will be necessary to answer the critical question in MTH: What is responsible for the zeolite-specific product distribution?

AUTHOR INFORMATION

Corresponding Author

*E-mail: abhan@umn.edu.

Notes

The authors declare no competing financial interest.

ACKNOWLEDGMENTS

The authors acknowledge financial support from Dow Chemical Company, the National Science Foundation (CBET 1055846), and the Abu Dhabi-Minnesota Institute for Research Excellence. Acknowledgment is also made to the donors of the American Chemical Society Petroleum Research Fund for partial support of this research. The authors acknowledge Mr. Ian Hill and Mr. Mark N. Mazar for helpful technical discussions.

REFERENCES

(1) Chang, C. D.; Silvestri, A. J. *J. Catal.* **1977**, *47*, 249−259.
(2) Hickman, D. A.; Schmidt, L. D. *Science* **1993**, *259*, 343−346.
(3) Laurendeau, N. M. *Prog. Energy Combust. Sci.* **1978**, *4*, 221−270.
(4) Wen, W. Y. *Catal. Rev. Sci. Eng.* **1980**, *22*, 1−28.
(5) Asadullah, M.; Ito, S.; Kunimori, K.; Yamada, M.; Tomishige, K. *J. Catal.* **2002**, *208*, 255−259.
(6) Sutton, D.; Kelleher, B.; Ross, J. R. H. *Fuel Process. Technol.* **2001**, *73*, 155−173.
(7) Dahl, I. M.; Kolboe, S. *Catal. Lett.* **1993**, *20*, 329−336.
(8) Dahl, I. M.; Kolboe, S. *J. Catal.* **1994**, *149*, 458−464.
(9) Dahl, I. M.; Kolboe, S. *J. Catal.* **1996**, *161*, 304−309.
(10) Ahn, J. H.; Temel, B.; Iglesia, E. *Angew. Chem.* **2009**, *121*, 3872−3874.
(11) Simonetti, D. A.; Ahn, J. H.; Iglesia, E. *J. Catal.* **2011**, *277*, 173−195.
(12) Mikkelsen, Ø.; Kolboe, S. *Microporous Mesoporous Mater.* **1999**, *29*, 173−184.
(13) Haw, J. F.; Song, W.; Marcus, D. M.; Nicholas, J. B. *Acc. Chem. Res.* **2003**, *36*, 317−326.
(14) Lesthaeghe, D.; Van Speybroeck, V.; Marin, G. B.; Waroquier, M. *Ind. Eng. Chem. Res.* **2007**, *46*, 8832−8838.
(15) Lesthaeghe, D.; Van Speybroeck, V.; Marin, G. B.; Waroquier, M. *Chem. Phys. Lett.* **2006**, *417*, 309−315.
(16) Song, W.; Marcus, D. M.; Fu, H.; Ehresmann, J. O.; Haw, J. F. *J. Am. Chem. Soc.* **2002**, *124*, 3844−3845.
(17) Marcus, D. M.; McLachlan, K. A.; Wildman, M. A.; Ehresmann, J. O.; Kletnieks, P. W.; Haw, J. F. *Angew. Chem. Int. Ed.* **2006**, *45*, 3133−3136.
(18) Ono, Y.; Mori, T. *J. Chem. Soc., Faraday Trans.* **1981**, *77*, 2209−2221.

(19) Langner, B. E. *Appl. Catal.* **1982**, *2*, 289−302.
(20) Dessau, R. M. *J. Catal.* **1986**, *99*, 111−116.
(21) Dessau, R. M.; LaPierre, R. B. *J. Catal.* **1982**, *78*, 136−141.
(22) Song, W.; Haw, J. F.; Nicholas, J. B.; Heneghan, C. S. *J. Am. Chem. Soc.* **2000**, *122*, 10726−10727.
(23) Mole, T.; Bett, G.; Seddon, D. *J. Catal.* **1983**, *84*, 435−445.
(24) Mikkelsen, O.; Ronning, P. O.; Kolboe, S. *Microporous Mesoporous Mater.* **2000**, *40*, 95−113.
(25) Tau, L. M.; Fort, A. W.; Bao, S.; Davis, B. H. *Fuel Process. Technol.* **1990**, *26*, 209−219.
(26) Bjørgen, M.; Svelle, S.; Joensen, F.; Nerlov, J.; Kolboe, S.; Bonino, F.; Palumbo, L.; Bordiga, S.; Olsbye, U. *J. Catal.* **2007**, *249*, 195−207.
(27) Svelle, S.; Joensen, F.; Nerlov, J.; Olsbye, U.; Lillerud, K.-P.; Kolboe, S.; Bjørgen, M. *J. Am. Chem. Soc.* **2006**, *128*, 14770−14771.
(28) Teketel, S.; Olsbye, U.; Lillerud, K.-P.; Beato, P.; Svelle, S. *Microporous Mesoporous Mater.* **2010**, *136*, 33−41.
(29) Hereijgers, B. P. C.; Bleken, F.; Nilsen, M. H.; Svelle, S.; Lillerud, K.-P.; Bjørgen, M.; Weckhuysen, B. M.; Olsbye, U. *J. Catal.* **2009**, *264*, 77−87.
(30) Bjørgen, M.; Joensen, F.; Lillerud, K.-P.; Olsbye, U.; Svelle, S. *Catal. Today* **2009**, *142*, 90−97.
(31) Svelle, S.; Olsbye, U.; Joensen, F.; Bjørgen, M. *J. Phys. Chem. C* **2007**, *111*, 17981−17984.
(32) Li, J.; Wei, Y.; Liu, G.; Qi, Y.; Tian, P.; Li, B.; He, Y.; Liu, Z. *Catal. Today* **2011**, *171*, 221−228.
(33) Cui, Z.-M.; Liu, Q.; Ma, Z.; Bian, S.-W.; Song, W.-G. *J. Catal.* **2008**, *258*, 83−86.
(34) Cui, Z. M.; Liu, Q.; Song, W. G.; Wan, L. J. *Angew. Chem. Int. Ed.* **2006**, *45*, 6512−6515.
(35) Teketel, S.; Skistad, W.; Benard, S.; Olsbye, U.; Lillerud, K. P.; Beato, P.; Svelle, S. *ACS Catal.* **2012**, *2*, 26−37.
(36) Teketel, S.; Svelle, S.; Lillerud, K.-P.; Olsbye, U. *ChemCatChem* **2009**, *1*, 78−81.
(37) Svelle, S.; Visur, M.; Olsbye, U.; Saepurahman, S.; Bjørgen, M. *Top. Catal.* **2011**, *54*, 897−906.
(38) Svelle, S.; Rønning, P. O.; Olsbye, U.; Kolboe, S. *J. Catal.* **2005**, *234*, 385−400.
(39) Svelle, S.; Rønning, P. O.; Kolboe, S. *J. Catal.* **2004**, *224*, 115−123.
(40) Hill, I. M.; Ng, Y. S.; Bhan, A. *ACS Catal.* **2012**, 1742−1748.
(41) Hill, I. M.; Hashimi, S. A.; Bhan, A. *J. Catal.* **2012**, *291*, 155−157.
(42) Hill, I. M.; Hashimi, S. A.; Bhan, A. *J. Catal.* **2012**, *285*, 115−123.
(43) Bercaw, J. E.; Diaconescu, P. L.; Grubbs, R. H.; Kay, R. D.; Kitching, S.; Labinger, J. A.; Li, X.; Mehrkhodavandi, P.; Morris, G. E.; Sunley, G. J.; Vagner, P. *J. Org. Chem.* **2006**, *71*, 8907−8917.
(44) Bercaw, J. E.; Diaconescu, P. L.; Grubbs, R. H.; Hazari, N.; Kay, R. D.; Labinger, J. A.; Mehrkhodavandi, P.; Morris, G. E.; Sunley, G. J.; Vagner, P. *Inorg. Chem.* **2007**, *46*, 11371−11380.
(45) Bercaw, J. E.; Grubbs, R. H.; Hazari, N.; Labinger, J. A.; Li, X. *Chem. Commun.* **2007**, 2974−2976.
(46) Bercaw, J. E.; Hazari, N.; Labinger, J. A.; Scott, V. J.; Sunley, G. J. *J. Am. Chem. Soc.* **2008**, *130*, 11988−11995.
(47) Simonetti, D. A.; Ahn, J. H.; Iglesia, E. *ChemCatChem* **2011**, *3*, 704−718.
(48) Van Speybroeck, V.; Van der Mynsbrugge, J.; Vandichel, M.; Hemelsoet, K.; Lesthaeghe, D.; Ghysels, A.; Marin, G. B.; Waroquier, M. *J. Am. Chem. Soc.* **2011**, *133*, 888−899.
(49) Svelle, S.; Tuma, C.; Rozanska, X.; Kerber, T.; Sauer, J. *J. Am. Chem. Soc.* **2009**, *131*, 816−825.
(50) Mazar, M. N.; Al-Hashimi, S.; Bhan, A.; Cococcioni, M. *J. Phys. Chem. C* **2012**, *116*, 19053−19612.
(51) Lesthaeghe, D.; Van Speybroeck, V.; Marin, G. B.; Waroquier, M. *Angew. Chem. Int. Ed.* **2006**, *45*, 1714−1719.
(52) Lee, C. C.; Gorte, R. J.; Farneth, W. E. *J. Phys. Chem. B* **1997**, *101*, 3811−3817.
(53) Stich, I.; Gale, J. D.; Terakura, K.; Payne, M. C. *J. Am. Chem. Soc.* **1999**, *121*, 3292−3302.
(54) Forester, T. R.; Howe, R. F. *J. Am. Chem. Soc.* **1987**, *109*, 5076−5082.
(55) Cheung, P.; Bhan, A.; Sunley, G. J.; Law, D. J.; Iglesia, E. *J. Catal.* **2007**, *245*, 110−123.
(56) Yamazaki, H.; Shima, H.; Imai, H.; Yokoi, T.; Tatsumi, T.; Kondo, J. N. *Angew. Chem. Int. Ed.* **2011**, *50*, 1−5.
(57) Bosacek, V. *J. Phys. Chem.* **1993**, *97*, 10732−10737.
(58) Wang, W.; Hunger, M. *Acc. Chem. Res.* **2008**, *41*, 895−904.
(59) Jiang, Y.; Hunger, M.; Wang, W. *J. Am. Chem. Soc.* **2006**, *128*, 11679−11692.
(60) Boronat, M.; Martinez, C.; Corma, A. *Phys. Chem. Chem. Phys.* **2011**, *13*, 2603−2612.
(61) Blaszkowski, S. R.; van Santen, R. A. *J. Phys. Chem. B* **1997**, *101*, 2292−2305.
(62) Blaszkowski, S. R.; van Santen, R. A. *J. Am. Chem. Soc.* **1996**, *118*, 5152−5153.
(63) Blaszkowski, S. R.; van Santen, R. A. *J. Phys. Chem.* **1995**, *99*, 11728−11738.
(64) Ivanova, II; Pomakhina, E. B.; Rebrov, A. I.; Hunger, M.; Kolyagin, Y. G.; Weitkamp, J. *J. Catal.* **2001**, *203*, 375−381.
(65) Weitkamp, J.; Jacobs, P. A.; Martens, J. A. *Appl. Catal.* **1983**, *8*, 123−141.
(66) Buchanan, J. S.; Santiesteban, J. G.; Haag, W. O. *J. Catal.* **1996**, *158*, 279−287.
(67) Frash, M. V.; Kazansky, V. B.; Rigby, A. M.; van Santen, R. A. *J. Phys. Chem. B* **1998**, *102*, 2232−2238.
(68) Rigby, A. M.; Kramer, G. J.; van Santen, R. A. *J. Catal.* **1997**, *170*, 1−10.
(69) Frash, M. V.; van Santen, R. A. *Top. Catal.* **1999**, *9*, 191−205.
(70) Hay, P. J.; Redondo, A.; Guo, Y. J. *Catal. Today* **1999**, *50*, 517−523.
(71) Kazansky, V. B.; Frash, M. V.; van Santen, R. A. *Stud. Surf. Sci. Catal.* **1997**, *105*, 2283−2290.
(72) Kazansky, V. B.; Frash, M. V.; van Santen, R. A. *Catal. Lett.* **1997**, *48*, 61−67.
(73) Boronat, M.; Viruela, P.; Corma, A. *J. Phys. Chem. B* **1999**, *103*, 7809−7821.
(74) Boronat, M.; Viruela, P.; Corma, A. *Phys. Chem. Chem. Phys.* **2000**, *2*, 3327−3333.
(75) Bao, S.; Tau, L. M.; Davis, B. H. *J. Catal.* **1988**, *111*, 436−439.
(76) Hazari, N.; Labinger, J. A.; Scott, V. J. *J. Catal.* **2009**, *263*, 266−276.
(77) Frash, M. V.; Solkan, V. N.; Kazansky, V. B. *J. Chem. Soc. Faraday Trans.* **1997**, *93*, 515−520.
(78) Boronat, M.; Viruela, P.; Corma, A. *J. Phys. Chem. A* **1998**, *102*, 9863−9868.
(79) Boronat, M.; Zicovich-Wilson, C. M.; Corma, A.; Viruela, P. *Phys. Chem. Chem. Phys.* **1999**, *1*, 537−543.
(80) Janik, M. J.; Davis, R. J.; Neurock, M. *J. Catal.* **2006**, *244*, 65−77.
(81) Mullen, G. M.; Janik, M. J. *ACS Catal.* **2011**, *1*, 105−115.
(82) Jasra, R. V.; Bhatt, B. D.; Garg, V. N.; Bhat, S. G. T. *Appl. Catal.* **1988**, *39*, 49−60.
(83) Dass, D. V.; Odell, A. L. *J. Catal.* **1988**, *113*, 259−262.
(84) Joshi, Y. V.; Thomson, K. T. *J. Catal.* **2005**, *230*, 440−463.
(85) Vandichel, M.; Lesthaeghe, D.; Van der Mynsbrugge, J.; Waroquier, M.; Van Speybroeck, V. *J. Catal.* **2010**, *271*, 67−78.
(86) Joshi, Y. V.; Thomson, K. T. *J. Phys. Chem. C* **2008**, *112*, 12825−12833.
(87) Ilias, S.; Bhan, A. *J. Catal.* **2012**, *290*, 186−192.
(88) Bjørgen, M.; Olsbye, U.; Petersen, D.; Kolboe, S. *J. Catal.* **2004**, *221*, 1−10.
(89) Van der Mynsbrugge, J.; Visur, M.; Olsbye, U.; Beato, P.; Bjørgen, M.; Van Speybroeck, V.; Svelle, S. *J. Catal.* **2012**, *292*, 201−212.
(90) Mirth, G.; Lercher, J. A. *J. Phys. Chem.* **1991**, *95*, 3736−3740.
(91) Saepurahman; Visur, M.; Olsbye, U.; Bjorgen, M.; Svelle, S. *Top. Catal.* **2011**, *54*, 1293−1301.

(92) Arstad, B.; Kolboe, S.; Swang, O. *J. Phys. Chem. B* **2002**, *106*, 12722−12726.
(93) Svelle, S.; Kolboe, S.; Olsbye, U.; Swang, O. *J. Phys. Chem. B* **2003**, *107*, 5251−5260.
(94) Svelle, S.; Kolboe, S.; Swang, O.; Olsbye, U. *J. Phys. Chem. B* **2005**, *109*, 12874−12878.
(95) Vos, A. M.; Nulens, K. H. L.; De Proft, F.; Schoonheydt, R. A.; Geerlings, P. *J. Phys. Chem. B* **2002**, *106*, 2026−2034.
(96) McCann, D. M.; Lesthaeghe, D.; Kletnieks, P. W.; Guenther, D. R.; Hayman, M. J.; van Speybroeck, V.; Waroquier, M.; Haw, J. F. *Angew. Chem. Int. Ed.* **2008**, *47*, 5179−5182.
(97) Mantha, R.; Bhatia, S.; Rao, M. S. *Ind. Eng. Chem. Res.* **1991**, *30*, 281−286.
(98) Rabiu, S.; Al-Khattaf, S. *Ind. Eng. Chem. Res.* **2008**, *47*, 39−47.
(99) Vinek, H.; Derewinski, M.; Mirth, G.; Lercher, J. A. *Appl. Catal.* **1991**, *68*, 277−284.
(100) Jentys, A.; Tanaka, H.; Lercher, J. A. *J. Phys. Chem. B* **2004**, *109*, 2254−2261.
(101) Pope, C. G. *J. Phys. Chem.* **1984**, *88*, 6312−6313.
(102) Lesthaeghe, D.; De Sterck, B.; Van Speybroeck, V.; Marin, G. B.; Waroquier, M. *Angew. Chem. Int. Ed.* **2007**, *46*, 1311−1314.
(103) UOP. http://www.uop.com/honeywells-uop-total-petrochemicals-successfully-demonstrate-technology-produce-plastics-feedstocks-oil/ (accessed Nov. 11, 2012).
(104) UOP. http://www.uop.com/honeywells-uop-methanoltoolefins-technology-selected-convert-coal-highvalue-petrochemicals-china/ (accessed Nov. 10, 2012).
(105) UOP. http://www.uop.com/honeywells-uop-wins-license-breakthrough-methanoltoolefins-mto-technology-convert-coal-highvalue-petrochemicals/ (accessed Nov. 10, 2012).
(106) Barger, P. T.; Vora, B. V.; Pujadó, P. R.; Chen, Q. *Stud. Surf. Sci. Catal.* **2003**, *145*, 109−114.
(107) Song, W.; Fu, H.; Haw, J. F. *J. Am. Chem. Soc.* **2001**, *123*, 4749−4754.
(108) Olsbye, U.; Svelle, S.; Bjørgen, M.; Beato, P.; Janssens, T. V. W.; Joensen, F.; Bordiga, S.; Lillerud, K. P. *Angew. Chem. Int. Ed.* **2012**, *51*, 5810−5831.
(109) Bjørgen, M.; Olsbye, U.; Svelle, S.; Kolboe, S. *Catal. Lett.* **2004**, *93*, 37−40.
(110) Xu, T.; Barich, D. H.; Goguen, P. W.; Song, W.; Wang, Z.; Nicholas, J. B.; Haw, J. F. *J. Am. Chem. Soc.* **1998**, *120*, 4025−4026.
(111) Bjørgen, M.; Olsbye, U.; Kolboe, S. *J. Catal.* **2003**, *215*, 30−44.
(112) Bjørgen, M.; Bonino, F.; Kolboe, S.; Lillerud, K.-P.; Zecchina, A.; Bordiga, S. *J. Am. Chem. Soc.* **2003**, *125*, 15863−15868.
(113) Wang, C. M.; Wang, Y. D.; Xie, Z. K.; Liu, Z. P. *J. Phys. Chem. C* **2009**, *113*, 4584−4591.
(114) Lesthaeghe, D.; Horré, A.; Waroquier, M.; Marin, G. B.; Van Speybroeck, V. *Chem.—Eur. J.* **2009**, *15*, 10803−10808.
(115) Lesthaeghe, D.; Van Speybroeck, V.; Waroquier, M. *Phys. Chem. Chem. Phys.* **2009**, *11*, 5222−5226.
(116) Sullivan, R. F.; Egan, C. J.; Langlois, G. E.; Sieg, R. P. *J. Am. Chem. Soc.* **1961**, *83*, 1156−1160.
(117) Xu, T.; Haw, J. F. *J. Am. Chem. Soc.* **1994**, *116*, 7753−7759.
(118) Stepanov, A. G.; Luzgin, M. V.; Arzumanov, S. S.; Ernst, H.; Freude, D. *J. Catal.* **2002**, *211*, 165−172.
(119) Luzgin, M. V.; Stepanov, A. G.; Arzumanov, S. S.; Rogov, V. A.; Parmon, V. N.; Wang, W.; Hunger, M.; Freude, D. *Chem.—Eur. J.* **2006**, *12*, 457−465.
(120) Long, J. F.; Wang, X. X.; Ding, Z. X.; Xie, L. L.; Zhang, Z. Z.; Dong, J. G.; Lin, H. X.; Fu, X. Z. *J. Catal.* **2008**, *255*, 48−58.
(121) Song, W. G.; Nicholas, J. B.; Haw, J. F. *J. Phys. Chem. B* **2001**, *105*, 4317−4323.
(122) Haw, J. F.; Nicholas, J. B.; Song, W.; Deng, F.; Wang, Z.; Xu, T.; Heneghan, C. S. *J. Am. Chem. Soc.* **2000**, *122*, 4763−4775.
(123) Sassi, A.; Wildman, M. A.; Ahn, H. J.; Prasad, P.; Nicholas, J. B.; Haw, J. F. *J. Phys. Chem. B* **2002**, *106*, 2294−2303.
(124) Sassi, A.; Wildman, M. A.; Haw, J. F. *J. Phys. Chem. B* **2002**, *106*, 8768−8773.
(125) Anderson, M. W.; Klinowski, J. *J. Am. Chem. Soc.* **1990**, *112*, 10−16.